Combined effects of cisplatin and photon or proton irradiation in cultured cells: radiosensitization, patterns of cell death and cell cycle distribution

Hiromitsu Iwata[1,2,*], Tsuyoshi Shuto[3], Shunsuke Kamei[3], Kohei Omachi[3], Masataka Moriuchi[3], Chihiro Omachi[4], Toshiyuki Toshito[4], Shingo Hashimoto[2], Koichiro Nakajima[1,2], Chikao Sugie[2], Hiroyuki Ogino[1,2], Hirofumi Kai[3] and Yuta Shibamoto[2]

[1]Department of Radiation Oncology, Nagoya Proton Therapy Center, Nagoya City West Medical Center, 1-1-1 Hirate-cho, Kita-ku, Nagoya 462-8508, Japan
[2]Department of Radiology, Nagoya City University Graduate School of Medical Sciences, 1 Kawasumi, Mizuho-cho, Mizuho-ku, Nagoya 467-8601, Japan
[3]Department of Molecular Medicine, Graduate School of Pharmaceutical Sciences, Kumamoto University, 5-1 Oe-honmachi, Chuo-ku, Kumamoto, 862-0973, Japan
[4]Department of Proton Therapy Physics, Nagoya Proton Therapy Center, 1-1-1 Hirate-cho, Kita-ku, Nagoya 462-8508, Japan
*Corresponding author. Department of Radiation Oncology, Nagoya Proton Therapy Center, Nagoya City West Medical Center, Nagoya, Japan, 1-1-1 Hirate-cho, Kita-ku, Nagoya 462-8508, Japan. Tel.: (+81) 52-991-8577; Fax: (+81) 52-991-8599; Email: h-iwa-ncu@nifty.com
(Received 10 April 2020; revised 22 June 2020; editorial decision 15 July 2020)

ABSTRACT

The purpose of the current study was to investigate the biological effects of protons and photons in combination with cisplatin in cultured cells and elucidate the mechanisms responsible for their combined effects. To evaluate the sensitizing effects of cisplatin against X-rays and proton beams in HSG, EMT6 and V79 cells, the combination index, a simple measure for quantifying synergism, was estimated from cell survival curves using software capable of performing the Monte Carlo calculation. Cell death and apoptosis were assessed using live cell fluorescence imaging. HeLa and HSG cells expressing the fluorescent ubiquitination-based cell cycle indicator system (Fucci) were irradiated with X-rays and protons with cisplatin. Red and green fluorescence in the G1 and S/G2/M phases, respectively, were evaluated and changes in the cell cycle were assessed. The sensitizing effects of ≥ 1.5 μM cisplatin were observed for both X-ray and proton irradiation ($P < 0.05$). In the three cell lines, the average combination index was 0.82–1.00 for X-rays and 0.73–0.89 for protons, indicating stronger effects for protons. In time-lapse imaging, apoptosis markedly increased in the groups receiving ≥ 1.5 μM cisplatin + protons. The percentage of green S/G2/M phase cells at that time was higher when cisplatin was combined with proton beams than with X-rays ($P < 0.05$), suggesting more significant G2 arrest. Proton therapy plus ≥ 1.5 μM cisplatin is considered to be very effective. When combined with cisplatin, proton therapy appeared to induce greater apoptotic cell death and G2 arrest, which may partly account for the difference observed in the combined effects.

Keywords: sensitizing effect; apoptosis; cell cycle; proton therapy; cisplatin; fluorescent ubiquitination-based cell cycle indicator system

INTRODUCTION

The application of proton therapy is expanding worldwide and its combination with chemotherapy is increasingly being investigated. Based on a relative biological effectiveness (RBE) of ∼1.1, proton beams are considered to exert similar biological effects to photons, and the same chemotherapy regimens and doses as those used in combination with X-ray treatments have been employed for proton therapy. However, the anti-tumor effects of proton beams when combined with concomitant chemotherapy have not yet been examined in detail. While the efficacy of chemo-proton therapy has been reported [1], severe adverse events
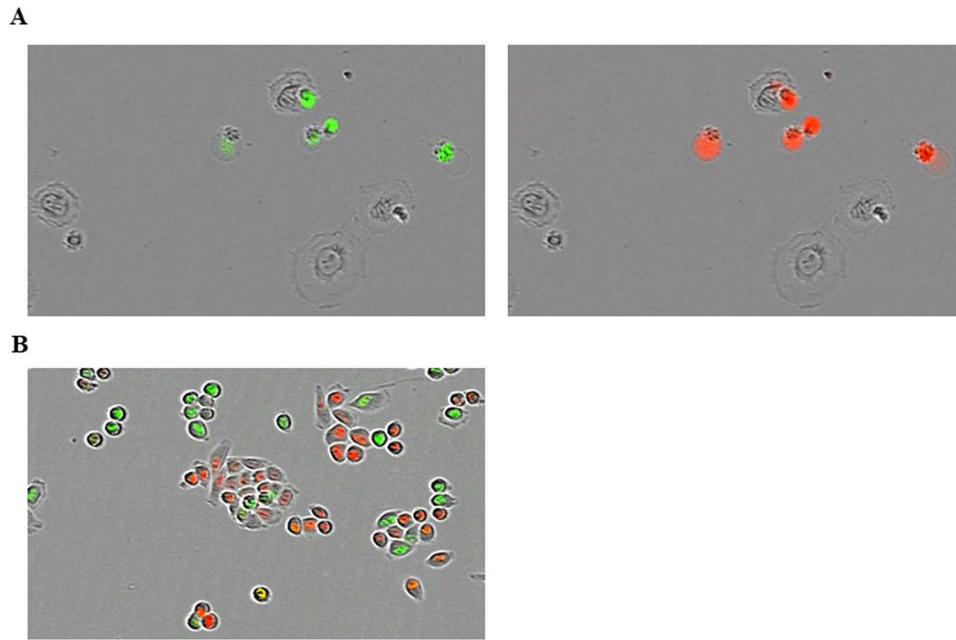
Fig. 1. (**A**) Example of the fluorescence of apoptotic EMT6 cells (green) and cell death (red) irradiated at 2 Gy by X-rays without cisplatin. In this image, some cells fluorescing in red also fluoresce in green; in these cells, it is considered that apoptosis led to death of the cells. (**B**) Example of the fluorescence of the HeLa/Fucci2 cell cycle. Red and green cells are in the G1 and S/G2/M phases, respectively.
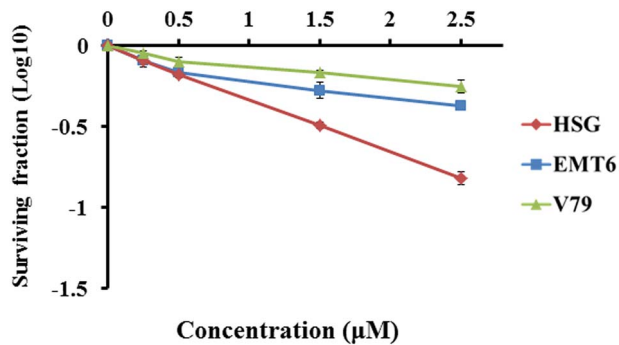

Fig. 2. Cell survival (plating efficiency) curves after treatments with 0.25–2.5 μM cisplatin alone. Bars represent standard errors of three experiments.

developed in patients receiving chemo-proton therapy [2]. Therefore, biological investigations on chemo-proton therapy are necessary and warranted [3, 4].

We have also been using chemotherapy in combination with proton therapy for locally advanced non-small-cell lung cancer, and cisplatin is a key drug in our regimen. Our initial findings have been favorable, and we observed the rapid shrinkage of lung cancer in patients treated with chemo-proton therapy [5]. Therefore, the effects of chemo-proton therapy, particularly the combination of cisplatin and protons, need to be investigated and compared with those of chemo-photon therapy. To account for the rapid shrinkage of tumors by chemo-proton therapy,

the patterns of cell death after cisplatin plus proton or X-ray treatments need to be clarified. Furthermore, since cisplatin exerts stronger sensitizing (synergistic) effects against protons than against X-rays, the effects of chemo-proton vs chemo-photon therapy on the cell cycle distribution should also be examined.

Fluorescent ubiquitination-based cell cycle indicator (Fucci) is a recently developed fluorescent probe for real-time observations of cell cycle progression in living cells [6]. Fucci visualizes cell cycles by fusing a fluorescent protein to two proteins, Geminin and Cdt1, which only appear during a specific cell cycle. Few studies have been conducted on the cell cycle distribution after proton irradiation and, to the best of our knowledge, none have been performed after chemo-proton therapy. Fucci allows for the elucidation of cell cycle-related biological phenomena, and may serve as a useful tool for examining the effects of proton therapy and developing optimal treatments (Supplementary Fig. 1, see online supplementary material).

In the present study, we evaluated the biological effects of protons and photons in combination with cisplatin in cultured cells and investigated the underlying mechanisms, including the patterns of cell death and effects on the cell cycle distribution, for each combination.

MATERIALS AND METHODS
Cells

Exponentially growing HSG human salivary gland tumor, EMT6 mouse mammary sarcoma, and V79 Chinese hamster lung fibroblast cells used in our previous study [7] were employed to evaluate sensitizing effects and patterns of cell death. The HSG cells (JCRB1070:
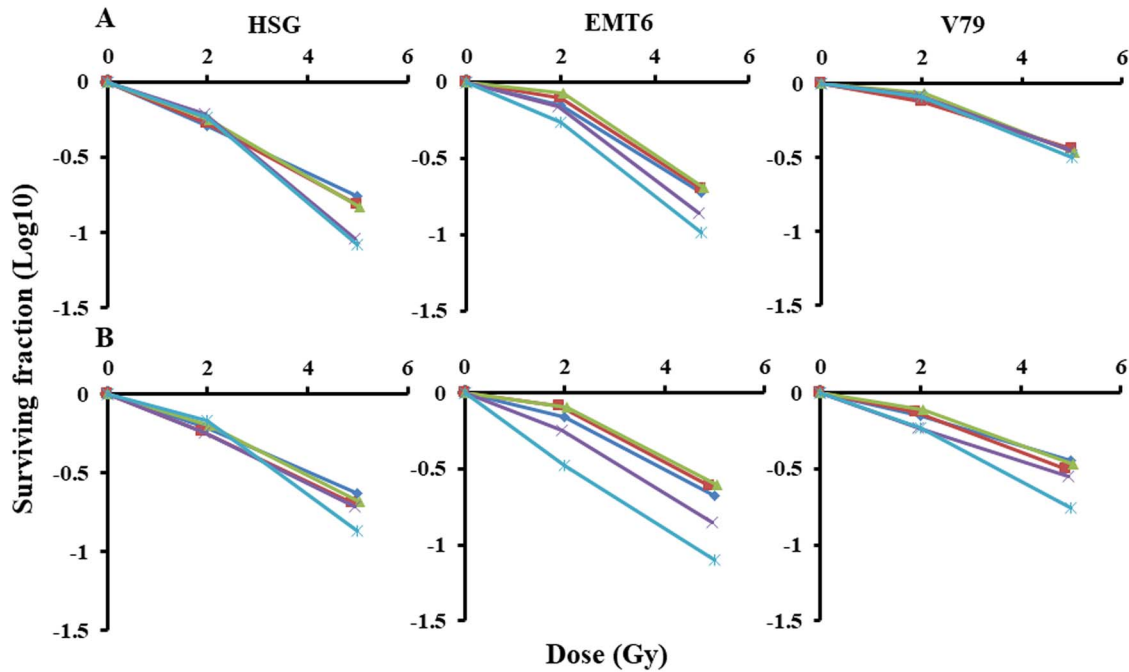
Fig. 3. Radiation dose–survival curves normalized by cisplatin toxicity. (A) X-Rays combined with cisplatin; (B) protons combined with cisplatin. Cisplatin concentrations: diamond, 0 μM; square, 0.25 μM; triangle, 0.5 μM; ×, 1.5 μM; ∗: 2.5 μM. Bars represent the standard errors of three experiments.

HSGc-C5) were kindly supplied by Drs Y. Hishikawa, T. Ogino and S. Nagayama (Medipolis Proton Therapy and Research Center, Kagoshima, Japan). Although this HSG cell line is contaminated with HeLa [8], it is a reference cell line used for comparisons of RBE among particle therapy facilities worldwide. These three cell lines were used because they had slightly different RBE values (1.01 [95% confidence interval: 1.00–1.03] for HSG, 1.15 [1.11–1.27] for EMT6 and 1.22 [1.06–1.29] for V79) [7].

As the standard cell line for Fucci studies, HeLa cells expressing Fucci (HeLa/Fucci2) provided by the RIKEN-BRC (Tsukuba, Japan) were used [6, 9]. In addition, HSG/Fucci was established in our laboratory by introducing mCherry and AmCyan1 into human HSG cells using the PiggyBac Transposon System (System Biosciences, Palo Alto, CA, USA) to evaluate the combined effects of radiation and cisplatin in the classically used cells in proton experiments [10]. A stable HSG/Fucci strain was prepared as follows. G1-Red and G2M-Cyan were amplified by PCR using a pTRE-cell cycle vector (Clontech, Palo Alto, CA, USA) as a template. The resulting G1-Red and G2M-Cyan were inserted into the PB-EF1-puro vector (PiggyBac system) to prepare two expression plasmid constructs: (1) G1-Red and (2) G2M-Cyan PB-EF1-puro vector. Cells transfected with (1) and (2) + Piggy-Bac transposase were selected with puromycin, followed by isolation and cultivation for G1-Red- and G2M-Cyan-double positive cells by fluorescence-activated cell sorting. To confirm whether dual monitoring (G1-Red and G2M-Cyan) worked in our established cells, we first used a fluorescence microscope. After visual checking, we sorted the cells to obtain dual stable HSG/Fucci. HeLa/Fucci2 cells were cultured in Dulbecco's modified Eagle's medium and the four other

cell lines were cultured in Eagle's minimum essential medium supplemented with 12.5% fetal bovine serum and antibiotics (100 U/ml penicillin and 100 μg/ml streptomycin); these media were used throughout the experiments. Cells were incubated in a humidified atmosphere with 5% CO_2 and 95% air at 37°C, and then subcultured on the day before experiments to maintain exponential growth.

Irradiation and cisplatin

Our proton therapy device and clinical results have already been reported in detail [11–13]. A dedicated jig (Masaki Corporation, Aichi, Japan) and solid phantom were used to ensure uniform physical doses of X-rays and protons. The irradiation field size was 10 × 10 × 10 cm. X-Ray irradiation was performed using Novalis-Tx (6 MV; Varian, Palo Alto, CA, and BrainLAB, Heimstetten, Germany) and spot-scanning proton beams with a 10-cm spread-out Bragg peak (SOBP) were generated using PROBEAT-III (Hitachi, Ltd., Tokyo, Japan; 152.6–200.5 MeV). X-Ray and proton irradiation were delivered at a dose rate of ~3.3 Gy/min. Physical doses were measured with the Advanced Markus Electron Chamber, PTW 34045 for protons and the PTW Farmer Chamber, Type 30013 for X-rays (PTW, Freiburg, Germany). These irradiation conditions were similar to those described in our previous experiments [7, 14].

Cisplatin obtained from SIGMA-ALDRICH (St. Louis, USA) was dissolved in sterile purified water and diluted with the medium. It was then added to the medium to yield a concentration of 0.25, 0.5, 1.5 or 2.5 μM. The former two concentrations were used as minimally toxic concentrations and the latter two as apparently toxic concentrations.

Table 1. CI of irradiation with cisplatin in the three cell lines. Data are presented as the mean of three determinations. The sensitizing effect is <1.0 in the CI [17]

Cell	Cisplatin (μM)	X-Ray + cisplatin		Proton + cisplatin	
		Dose (Gy)	CI	Dose (GyE)	CI
HSG	0.25	2	1.04	2	1.01
	0.5		1.12		1.12
	1.5		1.1		0.99
	2.5		0.82		0.86
	0.25	5	0.84	5	0.86
	0.5		0.79		0.83
	1.5*		0.48		0.68
	2.5		0.33		0.39
EMT6	0.25	2	1.21	2	1.47
	0.5		1.28		1.23
	1.5*		1		0.89
	2.5*		0.73		0.54
	0.25	5	0.94	5	1.04
	0.5		0.89		0.94
	1.5		0.68		0.62
	2.5*		0.55		0.4
V79	0.25	2	1	2	0.99
	0.5		1.19		0.98
	1.5*		1.23		0.67
	2.5*		1.08		0.61
	0.25*	5	0.97	5	0.8
	0.5*		0.88		0.78
	1.5*		0.88		0.63
	2.5*		0.74		0.38

*P < 0.05 between X-ray + cisplatin and proton + cisplatin.

Evaluation of sensitizing effects

We investigated the sensitizing effects of cisplatin against X-rays and proton beams. Six hours before each experiment, appropriate numbers of HSG, EMT6 and V79 cells were plated in flasks to create a scaffold. One hour before irradiation, cells were exposed to media containing 0–2.5 μM cisplatin and were then irradiated with single doses of 0–5 Gy/Gy equivalent (GyE) (RBE, 1.1) from X-rays and proton beams at the SOBP center under the same biological conditions, i.e. the same day, time and cell culture environment. One hour after irradiation, cisplatin was washed out from the medium. A standard colony assay was used to assess cell survival. In sensitization experiments, cell numbers in single-cell suspensions were counted after trypsinization using a TC10 automated cell counter (Bio-Rad Laboratories, Inc., Hercules, CA, USA) and appropriate numbers of cells were plated in triplicate for each point. The sensitizing effects and combination index (CI) [15] between each dose of irradiation and cisplatin were estimated from cell survival curves using the software CalcuSyn2 (Biosoft, Cambridge, UK), which is capable of performing the Monte Carlo calculation.

The CI is defined as follows:

$$(CI)_x = (D)_1/(D_x)_1 + (D)_2/(D_x)_2 = (D)_1/(D_m)_1[f_\alpha/(1-f_\alpha)]^{1/m1} + (D)_2/(D_m)_2[f_\alpha/(1-f_\alpha)]^{1/m2},$$

where $(Dx)_1$ is the dose of D1 (cisplatin concentration) alone that inhibits the growth of cells by x%, $(Dx)_2$ is the dose of D2 (radiation dose) alone that inhibits the growth of cells by x%, $(D)1$ and $(D)2$ are the doses of D1 and D2 in combination that also inhibit the growth of cells by x%. Dm is the median-effect dose, and f_α is the fraction affected. The CI value quantitatively defines synergism (<1), additive effects (1) and antagonism (>1) [15–17]. All experiments were performed three times.

Evaluation of the cell death pattern

As in the above experiment, 6 h before each experiment, appropriate numbers of HSG, EMT6 and V79 cells were plated on 96-well ImageLock Plates (Sartorius, Ann Arbor, Michigan) to create a scaffold. Cisplatin was then added, and irradiation was performed in the same manner. Appropriate amounts of reagents to dye dead cells (IncuCyte® Cytotox Red Reagent, Sartorius) and caspase-3/7 (IncuCyte Caspase-3/7 Green Apoptosis Assay Reagent, Sartorius) were added after washing out cisplatin, and time-lapse imaging was then performed using IncuCyte ZOOM 2015A (Sartorius) [18, 19]. The cell confluence ratio was calculated, and cell death and apoptosis were counted using live cell fluorescence imaging data. The confluence ratio was used to assess the optimal evaluation time and compare the fluorescence count (fluorescence count/image area) divided by the confluence ratio (cell area on the image/image area) under the same conditions. In each group, cells were seeded on 8 wells each, and four sites were photographed once every 4 h for each well. Data were obtained from the average value. Cytotoxicity at 52 h was then evaluated because the time for live cell confluence to reach 15–20%, which was a suitable condition for the experiment, was ∼52 h after irradiation. All experiments were performed three times. The proportion of apoptotic cells among dead cells was calculated by the ratio of fluorescence counts of apoptotic cells to fluorescence counts of cell death per cell area on the image. Figure 1A is an example of the fluorescence of apoptotic cells as well as dead cells including apoptotic cells.

Evaluation of the cell cycle distribution

We evaluated the RBE of HeLa/Fucci2 and HSG/Fucci cells using a standard colony assay. To examine the cell cycle, appropriate numbers of cells were plated on 96-well plates 6 h before each experiment. Cisplatin was then added, followed by irradiation with single doses of 0–8 Gy/GyE (RBE, 1.04) with X-rays or proton beams. One hour after irradiation, cisplatin was washed out of the medium. Red and green fluorescence in the G1 and S/G2/M phases, respectively, was counted every hour using IncuCyte Zoom. In the IncucyteZoom 2015A used in the present study, it is not possible to analyze orange cells. Cells near G1, near S, and in the middle show red, green, and both fluorescences, respectively. Since the number of colorless cells could not be accurately counted due to the overlapping of cells, the ratio of green cells to total cells could not be evaluated accurately. Changes in the cell cycle were then evaluated by simply calculating the proportion of green cells to red cells. Figure 1B is an example of the fluorescence of the cell cycle.

Statistical analysis

Curve fitting using the weighted least-squares method was performed using Kaleida Graph 4.5 (Hulinks, Tokyo, Japan) and CalcuSyn2.
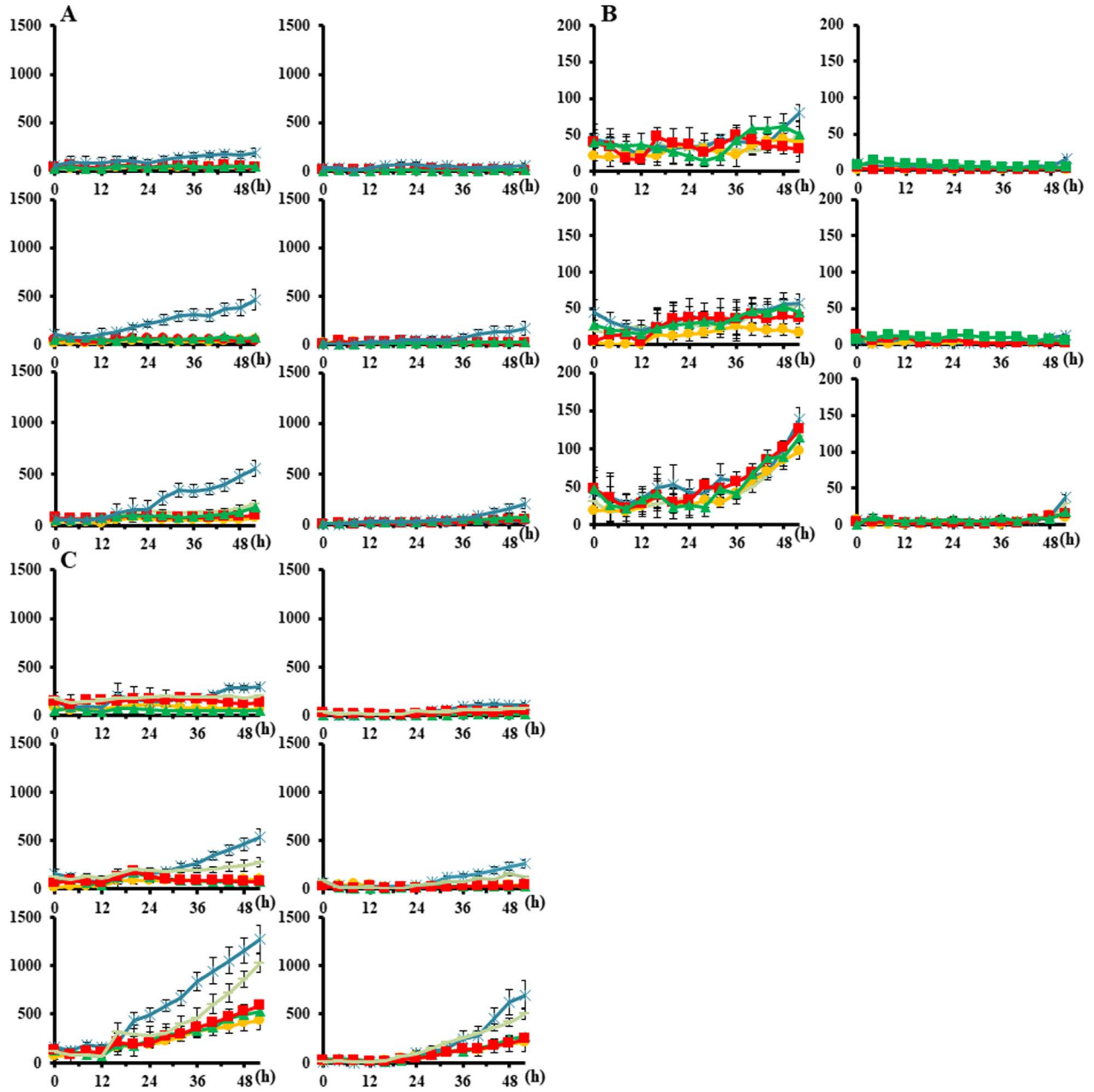
Fig. 4. Proportions of dead and apoptotic cells per cell area irradiated with X-rays. Bars represent the standard error of three experiments. circle, 0 μM, square; 0.25 μM; triangle, 0.5 μM; −, 1.5 μM; asterisk, 2.5 μM. (A) HSG, (B) EMT6 and (C) V79. The vertical axis indicates the number of counts per cell area on the image taken. The horizontal axis represents time (h). Left columns, cell death; right columns, apoptosis. Upper rows, control; middle rows, 2-Gy group; lower rows, 5-Gy group.

Statistical analyses were performed using SPSS 24.0 J (SPSS Japan Inc., Tokyo, Japan). In sensitization experiments, cell survival curves for the combination of cisplatin and X-rays or proton beams were normalized by cisplatin toxicities, and a two-way factorial analysis of variance was then performed to examine differences in survival curves between X-rays and proton beams. The Wilcoxon signed-rank test was used to compare combination indices with cisplatin for X-rays and proton beams and the proportion of apoptotic cells among dead cells between X-rays and protons in time-lapse imaging. Cell confluence ratios (G1 and S/G2/M phases) between X-rays and protons at the time at which most cells were arrested at G2 were compared by the paired *t*-test.
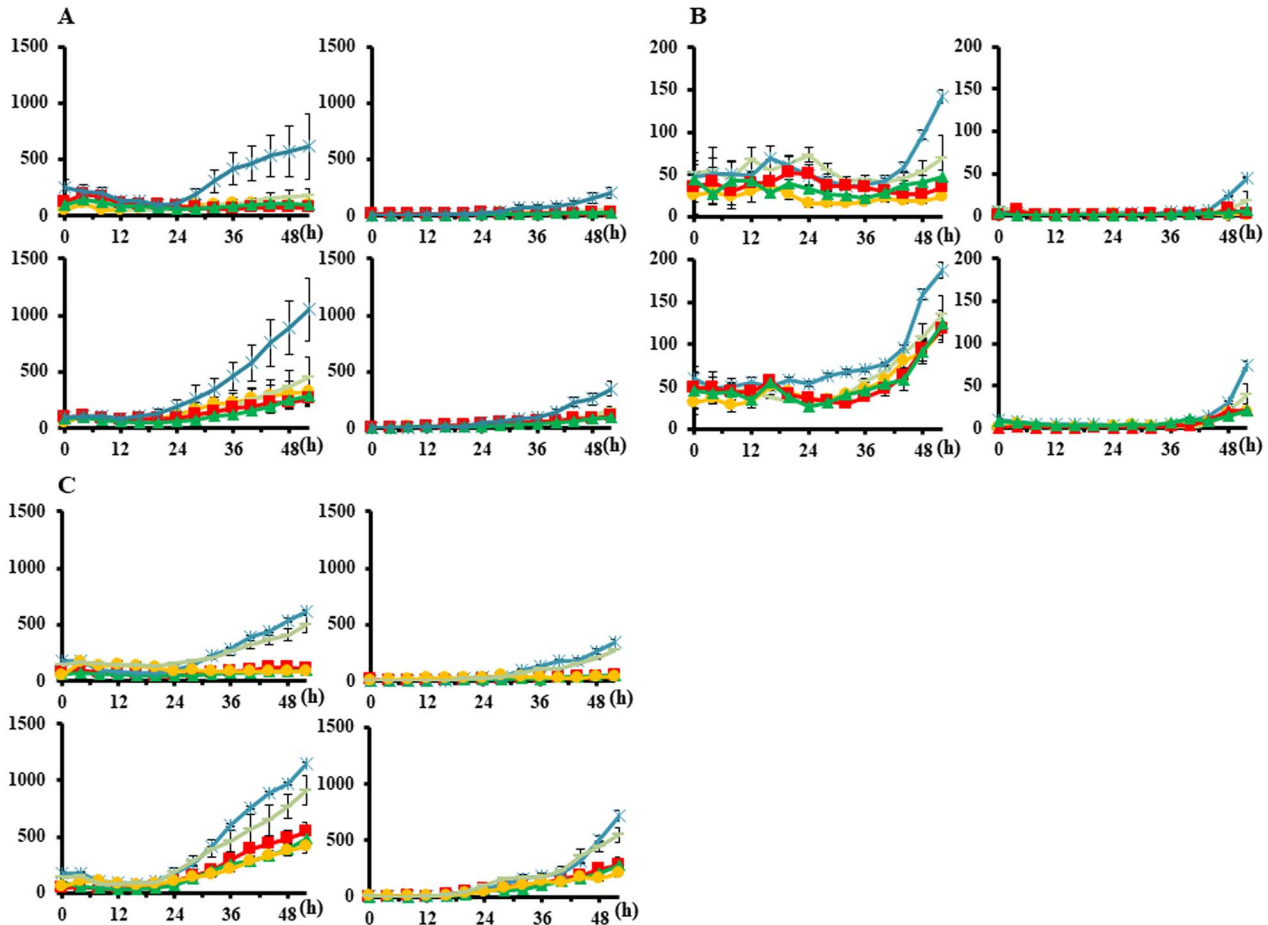
Fig. 5. Proportions of dead and apoptotic cells per cell area irradiated with proton beams. Bars represent the SD of three experiments. circle, 0 μM; square, 0.25 μM; triangle, 0.5 μM; −, 1.5 μM; asterisk, 2.5 μM. (A) HSG, (B) EMT6 and (C) V79. The vertical axis indicates the number of counts per cell area on the image taken. The horizontal axis represents time (h). Left columns, cell death; right columns, apoptosis. Upper rows, 2-GyE group; lower rows, 5-GyE group.

RESULTS

Cell surviving fractions after treatments with 0.25–2.5 μM cisplatin alone were 20–85%, 20–57% and 10–44% for HSG, EMT6 and V79, respectively (Fig. 2). Figure 3 shows radiation dose–survival curves for cisplatin-treated cells. The surviving fractions were normalized by cisplatin toxicity. Strong sensitizing effects were observed for X-rays and protons when combined with 1.5 or 2.5 μM cisplatin ($P < 0.05$). Supplementary Fig. 2, see online supplementary material, shows normalized isobolograms of irradiation with cisplatin. A normalized isobologram quantitatively assesses the non-constant ratio combinations (fixed-dose combinations) of two factors. The diagonal line is the line of additivity. Experimental data points (dots) located below, on and above the line indicate synergy, additivity and antagonism, respectively. Table 1 shows the combination indices of irradiation with cisplatin in the 3 cell lines: the average combination index in HSG, EMT6 and V79 cells was 0.82, 0.91 and 1.00, respectively, for X-rays and 0.84, 0.89 and 0.73, respectively, for protons, suggesting stronger effects for protons than for X-rays, particularly in EMT6 and V79.

The proportions of dead and apoptotic cells per cell area are shown in Figs 4 and 5. Table 2 shows the proportion of apoptotic cells among dead cells at 52 h for the three cell lines; the mean proportions were 37.9% (range, 33.2–41.9), 15.7% (6.2–27.4) and 47.7% (40.5–54.7) for the three cell lines, respectively, for X rays, and 34.4% (30.3–37.9), 20.5% (6.2–40.1) and 53.9% (44.9–63.0), respectively, for protons. No significant differences were observed in the cell death pattern in HSG between protons and X-rays in combination with cisplatin, whereas the proportion of apoptotic cells markedly increased in EMT6 and V79 after proton +1.5 or 2.5 μM cisplatin ($P < 0.05$).

The RBE (D10) was 1.04 (95% confidence interval: 1.01–1.07) for HeLa/Fucci2 and 1.04 (1.03–1.05) for HSG/Fucci (Supplementary Fig. 3, see online supplementary material). In time-lapse imaging, X-rays and proton beams both increased the ratio of green S/G2/M phase cells to red G1 phase cells after irradiation and delayed the cell cycle, suggesting G2 arrest (Fig. 6A). The proportion of green cells was increased slightly more by proton irradiation than by X-rays. The cell cycle delay as estimated by the time required to go over the peak of

Table 2. The proportion of apoptotic cells among dead cells at 52 h in the three cell lines. Data are presented as the mean and standard error of three determinations

Cell	Cisplatin (μM)	Control (%)	X-Ray 2 Gy (%)	Proton 2 GyE (%)	P value 2 Gy vs 2 GyE	X-Ray 5 Gy (%)	Proton 5 GyE (%)	P value 5 Gy vs 5GyE
HSG	0	19.1 ± 3.0	33.2 ± 3.1	30.3 ± 1.7	0.57	39.9 ± 1.6	36.3 ± 1.5	0.5
	0.25	19.8 ± 2.3	35.8 ± 0.7	31.5 ± 2.2	0.13	40.5 ± 2.6	36.4 ± 0.9	0.8
	0.5	21.8 ± 1.4	36.5 ± 0.8	34.9 ± 1.3	0.91	41.9 ± 2.6	37.9 ± 1.5	0.38
	1.5	29.6 ± 1.1	36.8 ± 0.6	32.6 ± 1.4	0.16	36.4 ± 2.5	33.1 ± 1.1	0.68
	2.5	31.0 ± 0.5	37.7 ± 1.0	33.1 ± 1.2	0.22	40.7 ± 1.5	37.4 ± 1.5	0.47
EMT6	0	4.2 ± 0.3	6.2 ± 1.2	6.2 ± 0.2	0.99	9.00 ± 1.1	15.7 ± 1.1	0.046
	0.25	6.0 ± 0.9	6.3 ± 1.4	6.5 ± 1.6	0.97	11.7 ± 0.8	17.6 ± 1.2	0.065
	0.5	6.7 ± 1.0	12.7 ± 1.7	15.2 ± 0.9	0.55	14.7 ± 1.1	16.4 ± 2.4	0.76
	1.5	17.3 ± 1.7	20.5 ± 1.2	25.9 ± 0.5	0.045	24.1 ± 0.4	29.4 ± 1.4	0.089
	2.5	25.0 ± 1.3	23.9 ± 1.3	31.8 ± 1.1	0.035	27.4 ± 2.0	40.1 ± 1.4	0.021
V79	0	26.2 ± 2.0	40.5 ± 0.9	44.9 ± 2.0	0.39	47.3 ± 1.1	51.5 ± 1.6	0.32
	0.25	31.7 ± 1.2	44.4 ± 1.4	48.7 ± 1.8	0.36	47.5 ± 1.2	52.9 ± 1.1	0.13
	0.5	30.0 ± 1.5	46.6 ± 2.0	50.4 ± 0.8	0.4	49.8 ± 1.2	57.4 ± 1.1	0.036
	1.5	35.9 ± 1.6	45.0 ± 1.7	54.9 ± 1.2	0.03	49.5 ± 1.8	60.0 ± 1.1	0.021
	2.5	36.4 ± 0.9	51.8 ± 1.4	55.7 ± 0.9	0.049	54.7 ± 1.0	63.0 ± 1.5	0.032

G2 arrest was prolonged by ~10 h after increasing the dose to 8 Gy. In addition, the cell cycle distribution after the initial G2 arrest exhibited no significant change due to the radiation dose or type (X-rays or protons). Even after the single administration of cisplatin, the proportion of green cells increased by 1–5-fold depending on the concentration of cisplatin, and it occurred at a later time (after 6–12 h) than G2 arrest caused by irradiation (Fig. 6, middle panels). The proportion of green cells at that time was higher when cisplatin was combined with proton beams than with X-rays in both cell lines ($P < 0.05$, Fig. 6, right panels). The decrease of the green cells after G2 arrest settled (at 12–24 h) after the combined treatment, suggesting the different effects of cisplatin and irradiation on the cell cycle.

DISCUSSION

Strong sensitizing effects were observed for X-rays and protons combined with 1.5 or 2.5 μM cisplatin; in EMT6 and V79, these effects were stronger with protons than with X-rays. This was not the case in HSG cells; however, this discrepancy may be explained in part by the low RBE (1.04) for HSG. Since EMT6 and V79 had higher RBEs (1.15 and 1.24, respectively) [7], biological doses to HSG were considered to be lower than those to EMT6 and V79. The mechanisms responsible for the effects of cisplatin and the interaction with X-rays have been studied by several groups [20–22]. Although, the RBE of proton beams is only slightly >1.0, a potential mechanism for radiosensitization is free radical-mediated, at least in part, leading to activated radiolytic species following the one-electron reduction of cisplatin. A second mechanism is biochemical in nature and involves the effects of cisplatin on cellular components via mechanisms that inhibit recovery from radiation-induced damage. The extent to which these reactions occur in a biological system currently remains unclear. Regarding the latter, the degree and type of DNA damage caused by irradiation as well as the distance between cisplatin-DNA adducts and the site of DNA damage caused by irradiation may be important. The differences between X-ray and proton beams in gene and protein expression due to various double-helix DNA cleavages and DNA response, and disorders during the process of cell death, have recently been reported [23, 24]. We previously reported that the contribution of indirect effects on DNA, as assessed by protection with dimethylsulfoxide, was less for proton beams than for X-rays in EMT6 cells [7]. Due to the greater contribution of direct effects than X-rays, the number of double-strand breaks increases, which further shortens the distance between cisplatin-DNA adducts and the site of DNA damage caused by irradiation. As a result, DNA damage repair may become difficult and cell killing effects may be enhanced. Grosse *et al.* [25] also reported that overall DNA damage differed between protons and X-rays, at least to a certain extent, requiring preferentially homologous recombination after proton irradiation than with X-ray irradiation. This result suggests a difference in the contribution of DNA repair types between protons and X-rays. The probability of an interaction is high and depends on the distance over which the two lesions interact and the probability of repair of the interacted lesion. We plan to biologically simulate this cleavage and interaction in the cell nucleus with GEANT-4 [26]. Unfortunately, a higher-RBE cell line in which the cell cycle distribution can be observed was not available for this study. In cells with a high RBE, the combination of cisplatin and proton beams may cause more DNA damage and more cell cycle arrest due to the need for repairing a larger amount of DNA damage, leading to cell cycle delay. Further evaluations with high-RBE cells are warranted. In addition, further studies using human lung cancer and esophageal cancer cells are also warranted in the future.

In live cell imaging, proton therapy combined with cisplatin yielded more apoptotic cells, which were observed at ~24–48 h after irradiation, not suggesting late cell death through a mitotic catastrophe [27, 28]. A possible reason for increased apoptosis, particularly with the combination of protons and cisplatin, is the involvement of mitochondria due to a p53 mutation or inactivation. A recent study reported that ionizing radiation stimulated mitochondrial oxidative phosphorylation (OXPHOS) in response to the energy requirement for DNA
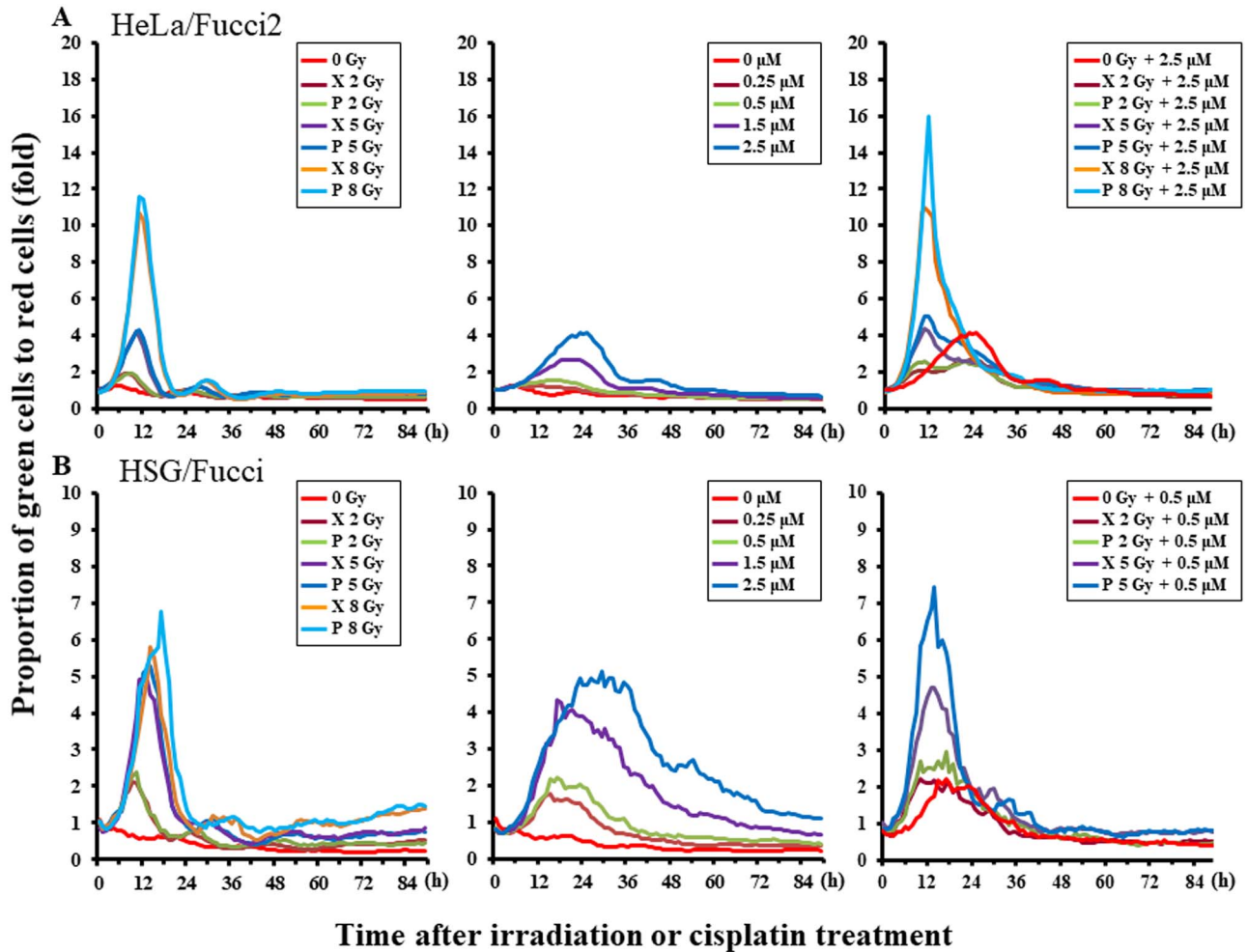
Fig. 6 Curves representing the ratio of green S/G2/M phase cells to red G1 phase cells after irradiation. (A) HeLa/Fucci2, (B) HSG/Fucci. Left panels, radiation alone; middle panels, cisplatin alone; and right panels, radiation combined with cisplatin. The groups of HSG/Fucci irradiated at 8 Gy or 8 GyE combined with 0.5 or 2.5 μM cisplatin were excluded from the right panels because the cell killing effect was too strong.

damage responses [29]. Reactive oxygen species (ROS) released during mitochondrial OXPHOS may cause oxidative damage to mitochondria in irradiated cells. Therefore, cytochrome c, which activates caspases, is released from mitochondria and translocates to the nucleus, causing DNA aggregation and fragmentation. It was also shown to be involved in the induction of apoptosis [30]. This pathway, i.e. effects on mitochondria, appears to be enhanced and the induction of apoptosis may be promoted. Mitteer *et al.* [31] also reported that proton radiation generated a larger quantity of ROS in glioma stem cells than X-rays. In addition, the rate of apoptosis was reported to be higher after proton irradiation than after X-rays [32]. The increase observed in apoptosis correlated with greater mitochondrial DNA damage and an increased mitochondrial mass, with prolonged oxidative stress and elevated protein oxidation after proton irradiation. These findings may in part support the increase in apoptosis observed in this experiment. Since apoptotic changes lead to rapid and complete cell disruption [33, 34], proton therapy combined with cisplatin may cause early tumor

shrinkage. This may lead to unexpected adverse events in normal tissues behind the tumor [35], and adaptive treatment planning appears to be mandatory. In the future, we will investigate changes in cellular organelles, such as mitochondrial membrane potential changes and ROS released during mitochondrial OXPHOS.

The present study revealed the absence of a significant difference in the cell cycle distribution between X-ray and proton irradiation alone, but showed an increase in G2 arrest after proton irradiation combined with cisplatin, suggesting more severe DNA damage or delayed DNA damage repair after combined therapy due to the G2 check-point system. Selective cytotoxicity to a specific cell cycle phase may lead to the synchronization of surviving cells. Since DNA repair by cisplatin requires a long time and living cells are synchronized more by proton irradiation, the cell killing effect is expected to be enhanced by split proton irradiation at the mitotic phase [36, 37]. In this experiment, an ∼1.5-fold increase in G2-arrested cells occurred in combination with protons compared with that with X-rays. Previous studies reported that

sublethal damage repair was inhibited by a combination of cisplatin and X-rays and also that potentially lethal damage repair was suppressed [38, 39]. We previously reported that sublethal damage repair was more efficiently inhibited by protons than by X-rays [13]. This may lead to a greater enhancement using fractionated proton irradiation combined with cisplatin. Optimal phases for administration and irradiation as well as the interval may be established using Fucci cells.

In conclusion, when combined with high concentrations of cisplatin, proton therapy appeared to be more effective than X-ray treatments; more apoptosis and a stronger G2 block were observed for the combination of proton therapy and cisplatin. Chronobiology may be applied to combination therapy with anticancer agents, such as cisplatin, in order to estimate optimal irradiation timing and dose fractionation.

SUPPLEMENTARY DATA

Supplementary data can be found at *RADRES Journal* online.

CONFLICT OF INTEREST

None declared.

REFERENCES

1. Chang JY, Verma V, Li M et al. Proton beam radiotherapy and concurrent chemotherapy for unresectable stage III non-small cell lung cancer: Final results of a phase 2 study. *JAMA Oncol* 2017;3:e172032.
2. Harada H, Fuji H, Ono A et al. Dose escalation study of proton beam therapy with concurrent chemotherapy for stage III non-small cell lung cancer. *Cancer Sci* 2016;107:1018–21.
3. Lühr A, von Neubeck C, Pawelke J et al. "radiobiology of proton therapy": Results of an international expert workshop. *Radiother Oncol* 2018;128:56–67.
4. Willers H, Allen A, Grosshans D et al. Toward a variable RBE for proton beam therapy. *Radiother Oncol* 2018;128:68–75.
5. Iwata H, Ogino H, Akita K et al. Tumor regression curve during and after concurrent chemotherapy and proton therapy for unresectable stage III non-small cell lung cancer: Comparison with chemo-x-radiation therapy. *Int J Radiat Oncol Biol Phys* 2016;96: E432–3.
6. Sakaue-Sawano A, Kobayashi T, Ohtawa K et al. Drug-induced cell cycle modulation leading to cell-cycle arrest, nuclear missegregation, or endoreplication. *BMC Cell Biol* 2011;12:2.
7. Iwata H, Ogino H, Hashimoto S et al. Spot scanning and passive scattering proton therapy: Relative biological effectiveness and oxygen enhancement ratio in cultured cells. *Int J Radiat Oncol Biol Phys* 2016;95:95–102.
8. Matsumoto Y, Matsuura T, Wada M et al. Enhanced radiobiological effects at the distal end of a clinical proton beam: In vitro study. *J Radiat Res* 2014;55:816–22.
9. Kaida A, Sawai N, Sakaguchi K et al. Fluorescence kinetics in HeLa cells after treatment with cell cycle arrest inducers visualized with Fucci (fluorescent ubiquitination-based cell cycle indicator). *Cell Biol Int* 2011;35:359–63.
10. Qi Z, Wilkinson MN, Chen X et al. An optimized, broadly applicable piggyBac transposon induction system. *Nucleic Acids Res* 2017 20;45:e55.
11. Toshito T, Omachi C, Kibe Y et al. A proton therapy system in Nagoya proton therapy center. *Australas Phys Eng Sci Med* 2016;39:645–54.
12. Iwata H, Toshito T, Hayashi K et al. Proton therapy for non-squamous cell carcinoma of the head and neck: Planning comparison and toxicity. *J Radiat Res* 2019;60:612–21.
13. Nakajima K, Iwata H, Ogino H et al. Acute toxicity of image-guided hypofractionated proton therapy for localized prostate cancer. *Int J Clin Oncol* 2018;23:353–60.
14. Hashimoto S, Sugie C, Iwata H et al. Recovery from sublethal damage and potentially lethal damage: Proton beam irradiation vs. X-ray irradiation. *Strahlenther Onkol* 2018;194:343–51.
15. Chou TC, Talalay P. Quantitative analysis of dose-effect relationships: The combined effects of multiple drugs or enzyme inhibitors. *Adv Enzyme Regul* 1984;22:27–55.
16. Shaw G, Prowse DM. Inhibition of androgen-independent prostate cancer cell growth is enhanced by combination therapy targeting hedgehog and ErbB signalling. *Cancer Cell Int* 2008;8: 3.
17. Chou TC. Drug combination studies and their synergy quantification using the Chou-Talalay method. *Cancer Res* 2010;70:440–6.
18. Chapman PJ, James DI, Watson AJ et al. IncucyteDRC: An R package for the dose response analysis of live cell imaging data. *F1000Res* 2016;5:962.
19. Artymovich K, Appledorn DM. A multiplexed method for kinetic measurements of apoptosis and proliferation using live-content imaging. *IncucyteMethods Mol Biol* 2015;1219:35–42.
20. Dewit L. Combined treatment of radiation and cisdiamminedichloroplatinum (II): A review of experimental and clinical data. *Int J Radiat Oncol Biol Phys* 1987;13:403–26.
21. Begg AC. Cisplatin and radiation: Interaction probabilities and therapeutic possibilities. *Int J Radiat Oncol Biol Phys* 1990;19:1183–9.
22. Douple EB. Cis-Diamminedichloroplatinum(II): Effects of a representative metal coordination complex on mammalian cells. *Pharmacol Ther* 1984;25:297–326.
23. Lühr A, von Neubeck C, Krause M, et al. Relative biological effectiveness in proton beam therapy - current knowledge and future challenges. *Clin Transl Radiat Oncol* 2018;9:35–41.

24. Carter RJ, Nickson CM, Thompson JM et al. Complex DNA damage induced by high linear energy transfer alpha-particles and protons triggers a specific cellular DNA damage response. *Int J Radiat Oncol Biol Phys* 2018;100:776–84.

25. Grosse N, Fontana AO, Hug EB et al. Deficiency in homologous recombination renders mammalian cells more sensitive to proton versus photon irradiation. *Int J Radiat Oncol Biol Phys* 2014;88:175–81.

26. de la Fuente Rosales L, Incerti S, Francis Z et al. Accounting for radiation-induced indirect damage on DNA with the Geant 4-DNA code. *Phys Med* 2018;51:108–16.

27. Kuwahara Y, Tomita K, Urushihara Y et al. Association between radiation-induced cell death and clinically relevant radioresistance. *Histochem Cell Biol* 2018;150:649–59.

28. Surova O, Zhivotovsky B. Various modes of cell death induced by DNA damage. *Oncogene* 2013;32:3789–97.

29. Shimura T, Sasatani M, Kawai H et al. A comparison of radiation-induced mitochondrial damage between neural progenitor stem cells and differentiated cells. *Cell Cycle* 2017;16:565–73.

30. Bröker LE, Kruyt FA, Giaccone G. Cell death independent of caspases: A review. *Clin Cancer Res* 2005;11:3155–62.

31. Mitteer R, Wang Y, Shah J et al. Proton beam radiation induces DNA damage and cell apoptosis in glioma stem cells through reactive oxygen species. *Sci Rep* 2015;5:13961.

32. Sertorio M, Köthe A, Perentesis J et al. Mitochondrial targeting may sensitize lymphoma cells to proton therapy. In: *Proceedings of the 58th Annual Meeting of the Particle Therapy Cooperative Group (PTCOG)*. 2019.

33. Wouters BG, Denko NC, Giaccia AJ et al. A p53 and apoptotic independent role for p21waf1 in tumour response to radiation therapy. *Oncogene* 1999;18:6540–5.

34. Brown JM, Wouters BG. Apoptosis, p53, and tumor cell sensitivity to anticancer agents. *Cancer Res* 1999;59:1391–9.

35. Patel D, Bronk L, Guan F et al. Optimization of Monte Carlo particle transport parameters and validation of a novel high throughput experimental setup to measure the biological effects of particle beams. *Med Phys* 2017;44:6061–73.

36. Grégoire V, Van NT, Stephens LC et al. The role of fludarabine-induced apoptosis and cell cycle synchronization in enhanced murine tumor radiation response in vivo. *Cancer Res* 1994;54:6201–9.

37. Gregoire V, Hittelman WN, Rosier JF et al. Chemo-radiotherapy: Radiosensitizing nucleoside analogues (review). *Oncol Rep* 1999;6:949–57.

38. Dritschilo A, Piro AJ, Kelman AD. The effect of cis-platinum on the repair of radiation damage in plateau phase Chinese hamster (V-79) cells. *Int J Radiat Oncol Biol Phys* 1979;5:1345–9.

39. Carde P, Laval F. Effect of cis-dichlorodiammine platinum II and X rays on mammalian cell survival. *Int J Radiat Oncol Biol Phys* 1981;7:929–33.